Article

Multiplexed in-Series Macro-Bend Fiber Sensors for Personal Authentication Through Foot Recognition

Natália Soares Girão[1] , Diogo Lugarini[1] , Lúcia Valéria Ramos de Arruda[1] , José Luís Fabris[1] , Marcia Muller[1]

[1]*Universidade Tecnológica Federal do Paraná, Campus Curitiba, Av. Sete de Setembro, 3165, Curitiba-PR, Brazil, 80230-901, soaresnatalia91@gmail.com, diogolugarini@gmail.com, lvrarruda@utfpr.edu.br, fabris@utfpr.edu.br, mmuller@utfpr.edu.br*

Abstract— **This work proposes a new tactile sensing system for biometric authentication. The system operates based on the response of multiplexed optical fiber macro-bend sensors to plantar pressure. The setup contains a set of 6 in-series sensors installed in holes drilled in a foot-shaped slab of Polymethyl Methacrylate. Each sensor is a loop of standard single-mode telecommunication fiber with 2.5 mm radius, encapsulated with silicone elastomer. The instrumentation required for interrogation includes only a broadband visible light source and a ultraviolet-visible spectrometer. Personal authentication is based on recognizing the unique pattern of pressures applied by the person's foot in the metatarsal, outside of the foot arch, and heel areas monitored by the 6 sensors. The light spectrum transmitted by the set of multiplexed sensors in the spectral range from 400 nm to 800 nm carries information about the magnitude of the pressure applied on each sensor by the foot. The distribution of pressures exerted by different individuals alters the geometry of the macro-bends, resulting in spectral changes in transmitted light that allow personal authentication. Principal component analysis and support vector machine method are responsible for foot recognition. Data analysis returned hit rates greater than 85% for 6 different feet.**

Index Terms— Biometric authentication, Multiplexed sensor, Optical fiber sensor, SVM

I. INTRODUCTION

Biometrics have attracted the attention of institutions and governments as a reliable method for personal authentication. Systems based on biometry designed for positive person identification can operate by comparing the individual captured biometric characteristic with that previously recorded and stored in a database or by searching the database for a match with recorded information of a set of individuals [1]. Setups based on capturing physiological and behavioral characteristics are safer than those based on traditional methods such as passwords, PINs, and cards, reducing the risk of fraud and justifying their use for human identification [2]. Whereas behavioral characteristics can change and not provide a unique recognition, physiological characteristics are considered constant over time [2]. Therefore, physiological characteristics such as those related to the shape of the human face, fingerprint, palmprint [3]–[5], and foot characteristics [1], [2], [6], among others, are promising candidates for a reliable human identification [2].

In the particular case of foot biometry, depending on the method used for the information extraction from the person's footstep, physiological and behavioral characteristics can be used for a person's authentication. Unique recognition of a person is obtained by recording, e.g., the foot geometry, the skin texture, the pressure distribution, and the gait characteristics [7]–[9].

To record the plantar pressure distribution, the use of commercially available platforms based on pressure sensors is widely spread. These equipment use arrays of resistive, capacitive, piezoelectric, or piezoresistive sensors to record pressure maps and other parameters of interest, such as maximum forces, pressures, and contact areas usually necessary in medical applications [10]. Some works proposed methods for personal recognition from the pressure distribution of the footprint measured with commercial pressure sensing mats [11], [12]. Traditional pressure sensors were also applied in pressure-sensitive sheets used as socks for biometric recognition from the gait features [13]. Despite representing a well-established technology, the required large number of sensors, the possible incidence of noise from the electrical equipment connecting data acquisition and processing systems, and the electrical wiring necessary for the proper system operation constitute some disadvantages of those systems. Some approaches suggest the use of footprint images captured by scanners [14] or recorded by cameras [7], [15], [16]. All these approaches require the use of methods of diverse complexity for data analysis or even data preprocessing to extract physiological or behavioral features such as foot shape and size and plantar pressure. Commercial platforms, scanners and in-shoe systems are usually used for static and dynamic indoor tests restricted to labs and clinics due to limitations for application in daily monitoring [10].

In an effort to overcome disadvantages related to traditional technologies, some works have proposed solutions based on optical fiber sensors (OFS). Over the past decades, the emergence of optical fiber communications has led to scientific findings and the development of new devices and equipment that promoted the popularization of optical fiber technologies. The success results from the optical fiber's unique characteristics as low cost, lightweight, small size, and immunity to electromagnetic interference. The sensing field is one of the most benefited from the advances in the area, and, nowadays, commercially available OFS are used in different sectors, replacing traditional technologies. There are numerous applications for this kind of sensor in fields where they can replace conventional sensors, emerging as solutions for limitations imposed by traditional technologies. OFS technology can explore the optical fiber's high sensitivity to physical and chemical parameters and the multiplexing ability, one of the most outstanding properties of these sensors, which allows only one interrogation unit to read information provided by a set of sensors. Multiplexing decreases the costs and complexity of sensing systems, making the OFS technology competitive. In order to address monitoring issues of different physical parameters over a single fiber link, multiplexing methods, such as spatial, time, or frequency division, have been proposed [17].

Over the years, the emergence of new applications and the need for monitoring large areas or simultaneously detecting different parameters further motivated the development of OFS systems, which resulted in a large amount of acquired data requiring the use of pattern recognition methods such as classification and/or clustering algorithms for data analysis [18].

In an attempt to explore the OFS favorable characteristics, fiber Bragg gratings [19]–[23], polymeric fiber devices and bend loss-based systems [24], [25] have been used as sensor elements in systems developed for plantar pressure monitoring. Some authors have developed different optical in-shoe plantar

pressure systems seeking reliable monitoring and other favorable characteristics such as portability, wearability, or wireless data acquisition [21], [22], [25], [26].

An overview of methods for personal authentication through foot recognition reported in the literature is summarized in Table I.

TABLE I. COMPARISON OF DIFFERENT METHODS FOR BIOMETRIC AUTHENTICATION FROM FOOTPRINTS

Data type	Equipment	Recognition Method	Accuracy	Ref.
Image	Pressure-sensitive mat	Euclidean distance	85%	[11]
Plantar pressure dynamic signal	Pressure-sensitive mat	HMM and LMA	64%	[12]
Image	Scanner	Cosine similarity	98.97%	[14]
Image	Digital camera	PCA and SVM	93.02%	[7]
Image	Apple iPhone	CNN/SqueezeNet	98.67%	[16]
Image	4 digital cameras	CNN/Deep learning	92.69%	[15]
Plantar pressure signal	Platform instrumented with FBG sensors	SVM algorithm	86.39%	[23]

Nakajima et al. [11] obtained an accuracy rate of 85%. However, the complex methodology used for analyzing the images obtained with a commercial pressure sensing mat involves many steps in the normalization procedure used to extract the geometric information from the raw image. The technique that uses as features the directionally aligned and quantized center of pressure trajectory during the human walk resulted in an average recognition rate of 64% even using the Hidden Markov Model (HMM) and the Levenberg-Marquardt Learning Algorithm (LMA) as methods [12]. Despite the low performance, the main contribution of the procedure is the use of dynamic images obtained during a walk.

The extraction of two features, shape and texture, from static images of naked footprints captured with a commercial scanner resulted in a higher recognition rate of 98.97% [14]. However, image preprocessing and distinct Gradient Vector Flow Snakes methods to extract the two features are required. Based on a threshold, a matching algorithm based on cosine similarity allows the process to decide how close the input and the identity data stored in a database must be. The user must be standing barefoot on the scanner, and the recognition depends on the capture of good quality images. It is worth to mention that the dataset used in these cited works was provided by commercial acquisition systems.

To avoid difficulties emerging from the diverse manners the person steps or walks that affect the plantar pressure distribution and the quality of the images provided by scanners, some authors have focused on the analysis of footprint or plantar images acquired by simpler acquisition data systems, such as digital cameras [7], or smartphones [16]. A method for intruder identification using images obtained with a digital camera that contains information on footprint morphology was proposed by [7]. PCA for pattern recognition and feature extraction and SVM to classify relevant classes resulted in an accuracy of 93.02%. Convolutional neural network (CNN) was used to classify individuals with an accuracy of 98.67% using plantar images obtained with a smartphone [16]. The work's main contribution was the use of the SqueezeNet technique, which allowed the automatic extraction of features from the images. Despite the high achieved recognition rates, the methods used in these works for recording foot images have limitations for real applications, and the development of appropriate acquisition systems is necessary.

Using an optical pedograph instrumented with 4 digital cameras for recording the footprint images and convolutional neural network trained with deep learning for the footprint classification a recognition rate

of 92.69% was achieved [15]. The training and validation test used footprint images from 16 volunteers. The biometric identification system consisting of a platform instrumented with FBGs returned hit hates greater than 86% [23]. The system has the advantage of requiring a small number of sensors (only 14) compared to commercial platforms. Besides, the SVM algorithm for pattern recognition requires low data preprocessing and low computational power. Recognition rates higher than 86% were obtained for 12 different stepping patterns used in the tests.

Among the OFS, those based on fiber macrocurvatures have been extensively used in different configurations and applications [26]–[33]. This class of sensors is particularly attractive owing to the simplicity of fabrication and interrogation. However, the ability of multiplexing a set of in-series macro-bends was only recently reported [33], unveiling new applications for this type of sensor. The interrogation of in-series multiplexed macro-bend sensors relies on wavelength-dependent intensity changes in the transmitted signal resulting from alterations induced by the external perturbation in the geometry of one or more sensors. These spectral modifications occur due to transition losses, pure bending losses, and resonances of whispering gallery modes (WGM). The coupled responses of 5 in-series macro-bend sensors installed under a steel plate (20 x 20 cm) divided into 16 sensing areas (5 x 5 cm) allowed the setup operation in quasi-distributed tactile sensing [34]. The tactile system provided the magnitude and location of a single load acting in one of the 16 pre-established sensing areas with an accuracy of 94.0%. The platform interrogation was based on the detection of the light spectrum transmitted by the in-series sensors when the platform was under load. As the sensors are under the plate, a single load acting in one sensing area can modify the geometry of more than one sensor. The complexity of the output signal required preprocessing with Principal Component Analysis (PCA) to reduce the dimensionality of the dataset presented to the predictive k-Nearest Neighbors (KNN) and Support Vector Machine (SVM) classification/regression models.

This paper proposes a biometric application using a different configuration for the multiplexed in-series macro-bend sensors previously reported [33], [34]. A foot-shaped Polymethyl Methacrylate (PMMA) slab was instrumented with 6 similar in-series macro-bend sensors and tested to detect 6 feet of different shapes and sizes. Unlike the sensing platform previously reported [34], where the sensors are under a steel plate, each sensor of the 6 in-series sensors is inserted in one hole of the foot-shaped slab. Therefore, the geometry of each sensor is modified by the pressure applied directly on its surface by the foot. As the output of one sensor is the input for the next one, the spectrum transmitted by the set of sensors carries information about the magnitude of the pressure applied on each sensor. Principal Component Analysis (PCA) and Support Vector Machine (SVM) were used to cluster similar foot allowing a pattern classification [35]. The application demonstrated here evaluated the feasibility of biometric personal authentication by recognizing the unique pattern of pressures produced by the person's foot. The sensing system and the data modeling are described in Section II. Typical spectral responses that contain the information used for biometric recognition, system repeatability, and performance are in Section III.

II. Methods

The developed sensing system contains a set of 6 in-series macro-bend sensors, each consisting of an optical fiber loop encapsulated at the center of a cylindrical silicone body. The fabrication method follows the steps previously described in [33]. The loops with a radius of $2.5\ mm$ were produced in the

Brazilian Microwave and Optoelectronics Society-SBMO   received 23 Nov 2023; for review 11 Dec 2023; accepted 01 Jun 2024

Brazilian Society of Electromagnetism-SBMag   © 2024 SBMO/SBMag   (cc) BY   ISSN 2179-1074

same segment of standard single-mode fiber (SSMF, G-652, Draktel, $1238\ nm$ cutoff wavelength). The loops were individually embedded in a silicone elastomer (Dow Corning, BX3-8001) for encapsulation using a mold. After the silicone cure, each sensor has a cylinder shape with a diameter of $21\ mm$ and height of $7\ mm$, containing the fiber loop approximately at its center. The plane formed by the fiber loop is orthogonal to the cylinder bases. Despite using the same procedure and parameters for fabrication, slight differences result in distinct sensors. The 6 in-series sensors are then inserted in circular holes drilled in a $5\ mm$ thick foot-shaped PMMA slab, as shown in Fig. 1. This configuration allows each sensor in the PMMA slab to detect pressure exerted exclusively on its surface, preventing the occurrence of coupled responses.

As a standard telecommunication optical fiber is used for sensor fabrication, interrogation in the spectral range from 400 to $800\ nm$ implies a multimodal operation regime. The experimental setup, shown in Fig. 1, contains a broadband white light source (LS-1 Tungsten Halogen, Ocean Optics) and a UV-VIS spectrometer (HR4000, Ocean Optics) in transmittance mode.

Static tests were performed by placing 6 feet of different shapes and lengths from $23\ cm$ to $27\ cm$ on the instrumented foot-shaped PMMA slab. The distribution of the sensors in the slab was chosen to monitor pressures applied in areas of interest for foot recognition. Such areas comprise the first metatarsal region, the outside of the foot arch, and the heel, as shown in Fig. 1 for one foot placed on the PMMA slab.
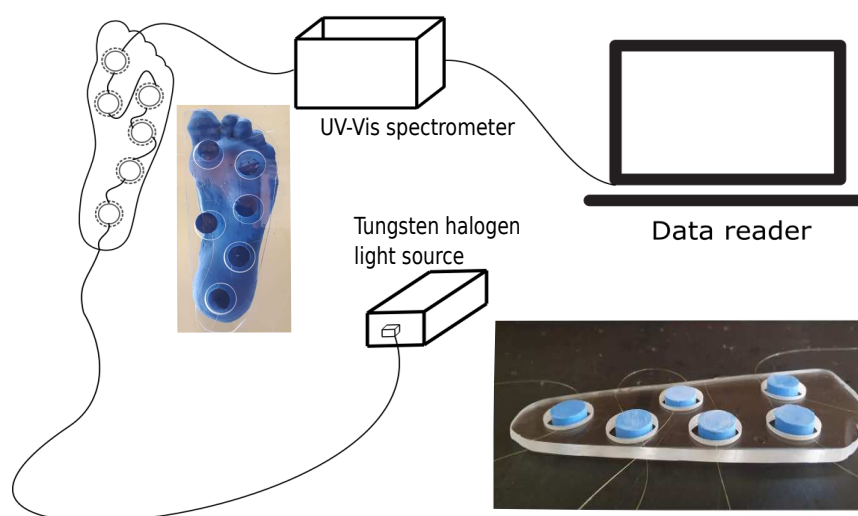

Fig. 1. Schematic diagram of the experimental setup; the foot-shaped PMMA slab instrumented with 6 in-series macro-bend sensors; a picture showing the foot areas monitored by the system when a foot is placed on the PMMA sheet.

For each foot, 10 transmission spectra were recorded, removing and placing the foot on the PMMA slab without trying to repeat precisely the previous position. Such intentional differences attempt to reproduce situations that may occur in field applications. The dataset composed of 60 transmission spectra (10 spectra per foot) in the spectral range from $400\ nm$ to $800\ nm$ was submitted to PCA and SVM methods. Due to the complexity of the dataset formed by the obtained spectra, PCA is used to reduce dimensionality by extracting the most relevant signal features. These features compose a new set of uncorrelated variables named principal components (PCs), which are easier to compute, reducing the complexity of the classification system [36]. The PCs form a vector basis, allowing clustering data that share similar information or characteristics, identifying regions for subsequent classification. The spectra

from the dataset obtained with the six different feet were normalized using the $z-score$ technique and processed by the PCA, following the procedure adopted in [33]. Using the two most relevant PCs allows data plotting in a two-dimensional graph, where each foot with different characteristics can be visually identified. From the reduced dimensionality dataset obtained after the PCA application, 90% was used for training and testing an SVM model with a gaussian kernel function. The remaining 10% was used for validating the model. The SVM kernel function can be generically represented by (1) supporting a multi-class algorithm [37].

$$G(x_1, x_2) = e^{(-\|x_1 - x_2\|^2)} \tag{1}$$

The validation model uses widely employed metrics to assert pattern recognition systems. For this, the obtained results are expressed not only in terms of accuracy but also in terms of Positive Predictive Value (*PPV*) and True Positive Rate (*TPR*), also known as precision and recall. Their complements, the False Negative Rate (*FNR*) and the False Detection Rate (*FDR*) are also computed.

While the recall provides the percentage of samples correctly identified out of the total examples of that class, the precision indicates the percentage of truly positive samples [38]. Additionally, the *F1-Score*, a metric that combines *PPV* and *TPR* in a harmonic mean (2), is used to evaluate the trained model.

$$F1 - Score = \frac{2 \times PPV \times TPR}{PPV + TPR} \tag{2}$$

III. RESULTS AND DISCUSSION

When one foot is placed on the instrumented foot-shaped slab, the pressure on each sensor produces a deformation in the silicone cylinder, affecting the internal fiber loop. As pure bend losses and light coupling from whispering gallery modes depend on the loop geometry, this alteration causes wavelength-dependent intensity changes in the spectrum of the light transmitted by the sensor. Since the set contains 6 in-series sensors, the light spectrum transmitted by one deformed sensor acts as the input for the next sensor. After the signal propagation through the whole set of sensors, the spectrometer records the resulting spectral modifications relatively to the spectrum transmitted by the unloaded system. Despite being fabricated with similar parameters, the sensors are slightly different. This characteristic makes the output signal dependent on the spatial distribution of pressures exerted by the foot. Therefore, feet with different shapes and sizes affect the set of sensors differently, resulting in dissimilar transmission spectra.

Fig. 2 shows representative pairs of transmission spectra resulting from each of the 6 different feet. These spectra exhibit wavelength-dependent intensity changes measured relatively to the unperturbed system used as a reference. The spectrum's shape is characteristic of each foot, as shown in Fig. 2, allowing biometric recognition of different individuals. The pairs of spectra associated with each foot exhibit in Fig. 2 qualitatively demonstrate the system repeatability. Regardless of the output signal complexity represented by the wavelength-dependent intensity changes, one specific foot produces similar spectra. Additionally, dissimilarities are observed when comparing spectra from different feet. These spectral differences contain information that assure biometric recognition.

It is important to emphasize that the dataset used for the foot recognition contains raw spectra recorded by consecutively removing and placing the foot on the measurement system without repeating

precisely the same position. This procedure, repeated 10 times for each foot, was adopted to simulate real situations occurring when, e.g., a person steps a footprint marker indicating the position for the biometric authentication. The number of repetitions and the inaccurate foot placement on the measurement system result in diverse but reliable data, which brings robustness to the trained model.
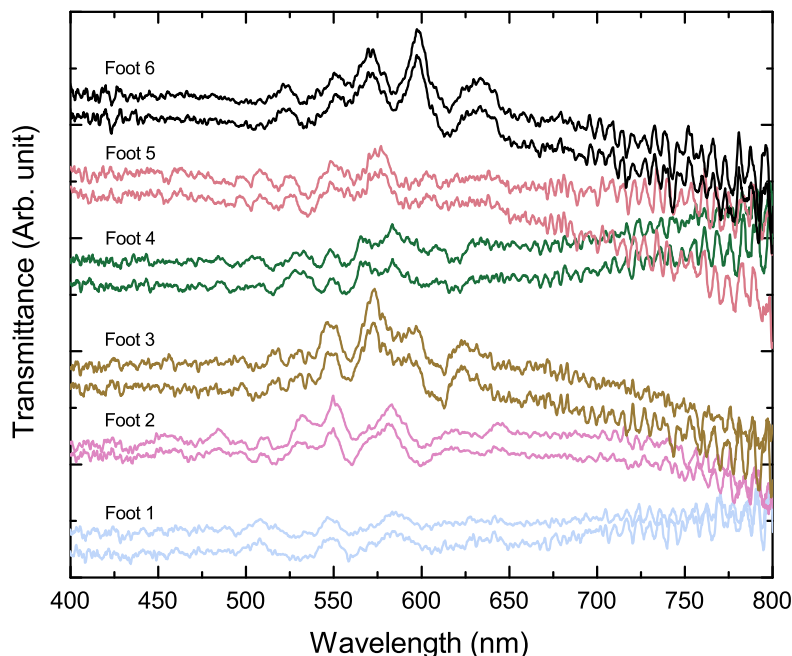

Fig. 2. Transmission spectra representative of the 6 different feet used in the experiments indicating the system reproducibility. The spectra are displayed with offsets for better visualization.

Fig. 3 shows spectra recorded under these conditions for the 6 feet resulting from 5 measurements. The spectral similarities observed for each foot indicate the system's robustness for real applications.

Fig. 4(a) shows the relevance of the first 10 PCs obtained for the raw dataset of 60 transmission spectra ranging from $400\ nm$ to $800\ nm$. This bar plot indicates that the information contained in the two first PCs is sufficient to characterize the samples, explaining about 65% of the data variance. Thus, the 2-dimensional dataset containing the two main PCs is built and shown in the graph of Fig. 4(b). As can be seen from this graph, measurements associated with the same foot share well-delimited regions for the first two major PCs. This result indicates the sensor's capability to differentiate the foot types under consideration, leading to a classification problem.

The 2-dimensional dataset resulting from PCA (60 data points in the graph of Fig. 4(b)) was used as an input for an SVM algorithm performed in Matlab, which resulted in an accuracy of 85.2% for testing data. For validation data (9 samples for each foot), the SVM model was able to classify correctly 100% of the samples. The confusion matrix for testing data is shown in Fig. 5. The true classes correspond to the matrix lines, while the matrix columns represent the classes predicted by the model. When the true class and the predicted class coincide, it is considered that the model made a correct prediction, and these values are shown in the main diagonal. For example, this confusion matrix shows that 6 samples of foot 3 are correctly classified, and the 3 other samples were erroneously classified as foot 6. This mismatching between classes 3 and 6 is also observed in Fig. 4(b), in which 2 samples from foot 3 (blue dot) are mixed with samples from foot 6 (pink dot).

On the right side of the confusion matrix in Fig. 5, there are the Recall (or True Positive Rate) and

the False Negative Rate, while at the bottom are the Precision (or Positive Predictive Value) and the False Detection Rate. These values can also be found with their respective resulting *F1-Score* for each class in Table II. It is worth mentioning that the dataset preprocessing requires only the application of a simple method based on PCA that favors the use of the proposed approach in a real-time personal authentication system.
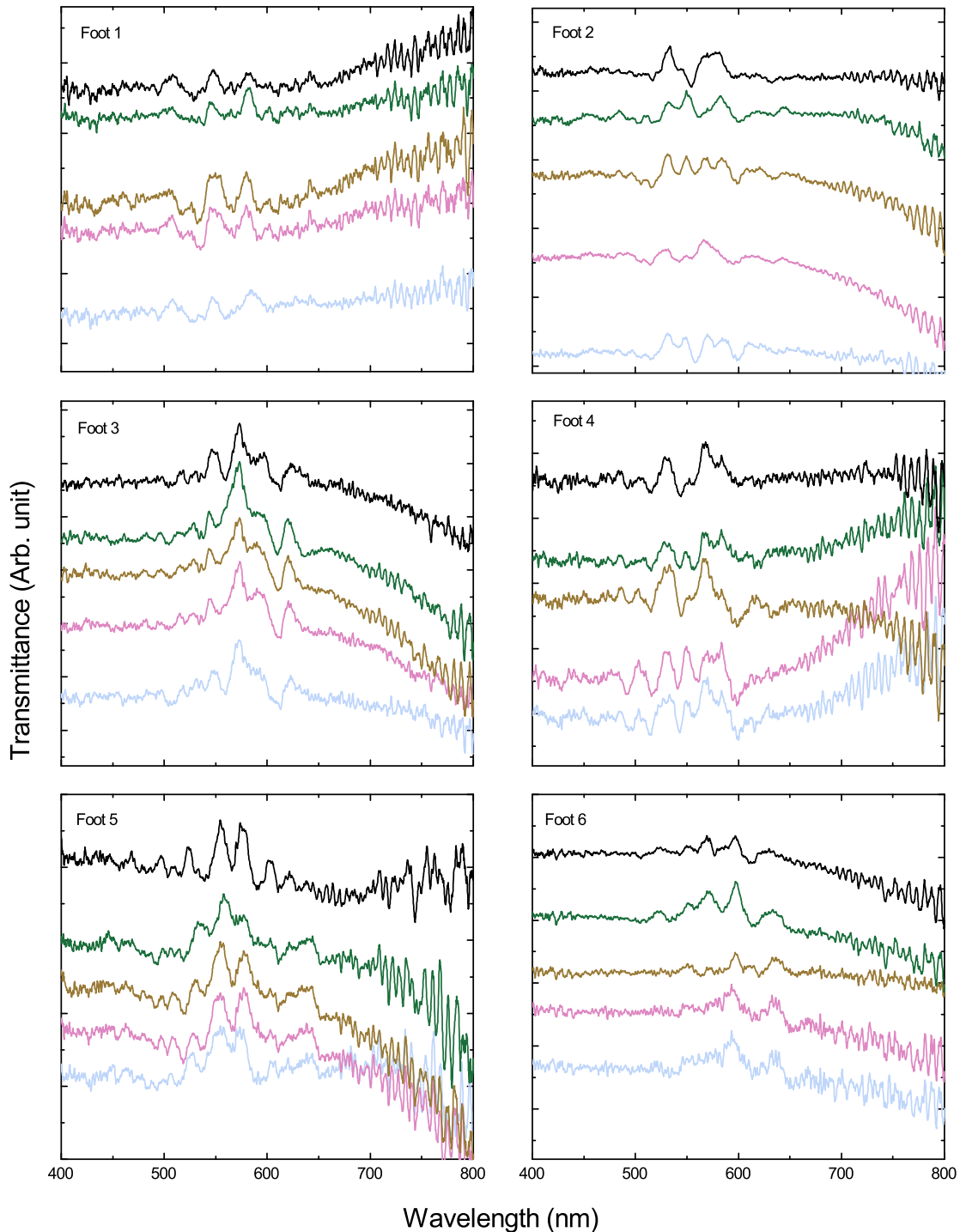

Fig. 3. Transmission spectra obtained for each foot without repeating exactly the same foot placement on the PMMA slab, indicating the system robustness for real applications.

In addition to what can be visually inferred from Fig. 4(b), the highest values for *F1-Scores*, associated

with feet 2 and 4, indicate that these are the most distinguishable feet among the 6 belonging to the dataset. Furthermore, the two classes that tend to be the most confused are the ones corresponding to feet 3 and 6. It can be inferred that the confusion comes from a certain level of similarity in the format of the considered feet.
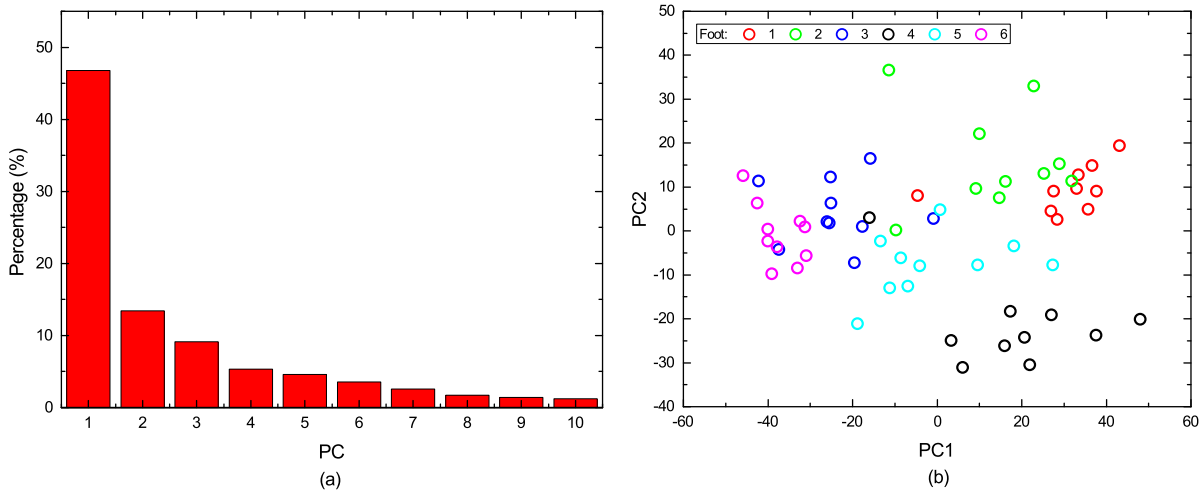

Fig. 4. Results of Principal Component Analysis: (a) Percentage of variance explained by the 10 first PCs, (b) Data from each foot represented by the first 2 PCs.
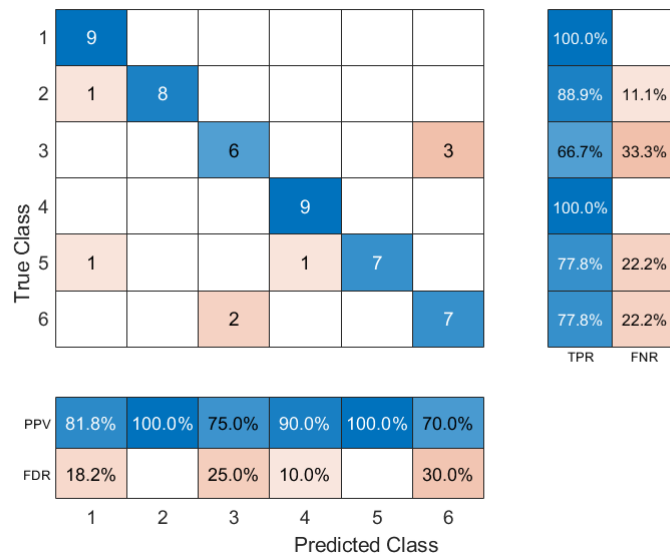

Fig. 5. Gaussian SVM confusion map for testing data.

The tactile sensing system based on optical fiber macro-bend sensors of this work show an accuracy of over 85%, which is comparable with some of the works in Table I. Additionally, it has some advantages compared to the methods found in the literature, offering a promising alternative for biometric authentication. It requires a small number of sensors and simple instrumentation for data acquisition. The set of in-series sensors can be installed in different configurations and are cheap and easy to fabricate. Regarding data processing, PCA efficiently reduces the dataset dimensionality and extracts the most relevant signal features from the raw spectrum. No additional preprocessing method is required. Furthermore, the SVM algorithm offers a well-established and efficient approach, potentially

reducing complexity compared to Deep Learning model techniques.

TABLE II. PRECISION, RECALL AND F1-SCORES FOR EACH CLASS

Class	Precision	Recall	F1 Score
1	1	0.818	0.8999
2	0.889	1	0.9412
3	0.667	0.750	0.7061
4	1	0.900	0.9474
5	0.778	1	0.8751
6	0.778	0.700	0.7369

IV. CONCLUSION

This work shows the possibility of biometric authentication through foot recognition with a system based on multiplexed macro-bend sensors. The output signal of only 6 similar sensors distributed in a spatial configuration chosen to monitor pressures exerted by the foot in the metatarsal, heel, and outside the foot arch areas allowed personal authentication. Besides the advantage of using a small number of multiplexed sensors, the in-series macrobends that constitute the system are easy to fabricate using standard optical fibers and an ordinary elastomer as encapsulating material. The low complexity of the fabrication process results in a versatile set of sensors. These sensors can be easily installed in a configuration adequate for the desired application. Another advantage is the interrogation using ordinary equipment for UV-Vis spectroscopy, a well-established technology.

The system operates in a multimodal regime as the sensors are fabricated using standard SMF fibers and the interrogation is within the $400\ nm$ to $800\ nm$ range. This particular characteristic results in complex modifications in the transmission spectra due to bend losses and WGM, which are related to the features of the foot. Consequently, the quality and amount of information carried by the transmission spectra allows foot recognition and, therefore, biometric authentication. Despite the complexity of the spectral modifications associated with the characteristics of each foot, the method combining PCA and SVM techniques used for the data analysis extracted features from the spectra that allowed the feet to be distinguished. The SVM, an easily applicable and low-cost computational algorithm, managed to classify the reduced dataset from PCA, plotted as data points in a bi-dimensional space, with an accuracy of over 85% for essayed data. Future works can evaluate the robustness of the proposed approach increasing the dataset using a large variety of feet. Besides, the performance can also be evaluated with a configuration containing two foot-shaped slabs and a larger number of sensors to record information of footprints of a person standing on both feet. Some possible sources of error that might affect the sensor's performance should be considered when projecting a commercial equipment. The effect of intensity fluctuations of the light source can be minimized by taking a reference spectrum for the spectrometer right before acquiring the spectrum corresponding to the foot under authentication. For long-term thermal changes in the environment where the sensor is installed, a previous calibration considering this parameter can be incorporated to compensate for these changes. As the elastomer used for encapsulating the fiber loop has low thermal conductivity (about 1 W/m/K), the impact of short-term thermal fluctuations is of minor concern. Additionally, changes in the mechanical properties of the elastomer from repetitive use might impair the sensor's performance, leading to the need for recalibration or even replacement of the sensors.

ACKNOWLEDGMENTS

REFERENCES

[1] K. M. Hashem and F. Ghali, "Human identification using foot features," *International Journal of Engineering and Manufacturing*, vol. 6, no. 4, pp. 22–31, 2016.

[2] R. Kushwaha, N. Nain, and S. K. Gupta, "Person Identification on the Basis of Footprint Geometry," in *2016 12th International Conference on Signal-Image Technology & Internet-Based Systems (SITIS)*, pp. 164–171, 2016. [Online]. Available: http://ieeexplore.ieee.org/document/7907461/

[3] H. C. S. A. Kumar, D. C. M. Wong and A. K. Jain, "Personal verification using palmprint and hand geometry biometric," in *In Proceedings of the 4th International Conference on Audio-and Video-Based Biometric Person Authentication*, pp. 668–678, 2006.

[4] B. S. E. Yoruk, E. Konokoglu and J. Darbon, "Shape-based hand recognition," *IEEE Transaction on Image Processing*, vol. 15, pp. 1803–1815, 2006.

[5] R. Sanchez-Reillo, C. Sanchez-Avila, and A. Gonzalez-Marcos, "Biometric identification through hand geometry measurements," *IEEE Transactions on Pattern Analysis and Machine Intelligence*, vol. 22, no. 10, pp. 1168–1171, 2000. [Online]. Available: http://ieeexplore.ieee.org/document/879796/

[6] A. Uhl and P. Wild, "Personal identification using Eigenfeet, Ballprint and Foot geometry biometrics," in *Proceedings of the First IEEE International Conference on Biometrics: Theory, Application, and Systems 2007 (IEEE BTAS'07)*, pp. 1–6, 2007.

[7] V. D. Ambeth Kumar, V. D. Ashok Kumar, S. Malathi, and P. Jagaeedesh, "Intruder Identification Using Footprint Recognition with PCA and SVM Classifiers," *Advanced Materials Research*, vol. 984-985, pp. 1345–1349, 2014.

[8] E. Liu, "Infant Footprint Recognition," in *2017 IEEE International Conference on Computer Vision (ICCV)*, pp. 1662–1669, 2017.

[9] V. Dhir, A. Singh, R. Kumar, and G. Singh, "Biometric recognition: a modern era for security," *International Journal of Engineering Science and Technology*, vol. 2, no. 8, pp. 3364–3380, 2010.

[10] A. H. A. Razak, A. Zayegh, R. K. Begg, and Y. Wahab, "Foot plantar pressure measurement system: A review," *Sensors*, vol. 12, no. 7, pp. 9884–9912, 2012. [Online]. Available: https://www.mdpi.com/1424-8220/12/7/9884

[11] K. Nakajima, Y. Mizukami, K. Tanaka, and T. Tamura, "Footprint-based personal recognition," *IEEE Transactions on Biomedical Engineering*, vol. 47, no. 11, pp. 1534–1537, 2000. [Online]. Available: http://ieeexplore.ieee.org/document/880106/

[12] J.-W. Jung, Z. Bien, S.-W. Lee, and T. Sato, "Dynamic-footprint based person identification using mat-type pressure sensor," in *Proceedings of the 25th Annual International Conference of the IEEE Engineering in Medicine and Biology Society (IEEE Cat. No.03CH37439)*, vol. 3, pp. 2937–2940, 2003. [Online]. Available: https://ieeexplore.ieee.org/document/1280533/

[13] T. Yamakawa, K. Taniguchi, K. Asari, S. Kobashi, and Y. Hata, "Biometric personal identification based on gait pattern using both feet pressure change," in *2008 World Automation Congress*, pp. 1–6, 2008.

[14] R. R. King and W. Xiaopeng, "Study of Biometric Identification Method Based on Naked Footprint," *International Journal of Science and Engineering*, vol. 5, no. 2, pp. 29–35, 2013. [Online]. Available: http://ejournal.undip.ac.id/index.php/ijse/article/view/5511

[15] T. Keatsamarn and C. Pintavirooj, "Footprint Identification using Deep Learning," in *2018 11th Biomedical Engineering International Conference (BMEiCON)*, pp. 1–4, 2018. [Online]. Available: https://ieeexplore.ieee.org/document/8609926/

[16] S. I. Safie and R. Ramli, "Footprint biometric authentication using SqueezeNet," *Indonesian Journal of Electrical Engineering and Computer Science*, vol. 31, no. 2, p. 893, 2023. [Online]. Available: https://ijeecs.iaescore.com/index.php/IJEECS/article/view/29478

[17] J. P. Dakin, "Multiplexed and distributed optical fibre sensor systems," *Journal of Physics E: Scientific Instruments*, vol. 20, no. 8, pp. 954–967, 1987.

[18] A. Venketeswaran, N. Lalam, J. Wuenschell, P. R. Ohodnicki, M. Badar, K. P. Chen, P. Lu, Y. Duan, B. Chorpening, and M. Buric, "Recent Advances in Machine Learning for Fiber Optic Sensor Applications," *Advanced Intelligent Systems*, vol. 4, no. 1, p. 2100067, 2022.

[19] A. Guru Prasad, S. Omkar, H. Vikranth, V. Anil, K. Chethana, and S. Asokan, "Design and development of Fiber Bragg Grating sensing plate for plantar strain measurement and postural stability analysis," *Measurement*, vol. 47, pp. 789–793, 2014. [Online]. Available: https://linkinghub.elsevier.com/retrieve/pii/S0263224113004909

[20] R. Suresh, S. Bhalla, J. Hao, and C. Singh, "Development of a high resolution plantar pressure monitoring pad based on fiber Bragg grating (FBG) sensors," *Technology and Health Care*, vol. 23, no. 6, pp. 785–794, 2015. [Online]. Available: https://www.medra.org/servlet/aliasResolver?alias=iospress&DOI=10.3233/THC-151038

[21] C. Tavares, M. Domingues, A. Frizera-Neto, T. Leite, C. Leitão, N. Alberto, C. Marques, A. Radwan, E. Rocon, P. André, and P. Antunes, "Gait Shear and Plantar Pressure Monitoring: A Non-Invasive OFS Based Solution for e-Health Architectures," *Sensors*, vol. 18, no. 5, p. 1334, 2018. [Online]. Available: http://www.mdpi.com/1424-8220/18/5/1334

[22] M. F. Domingues, N. Alberto, C. S. J. Leitão, C. Tavares, E. R. de Lima, A. Radwan, V. Sucasas, J. Rodriguez, P. S. Andre, and P. F. Antunes, "Insole optical fiber sensor architecture for remote gait analysis—an e-health solution," *IEEE Internet of Things Journal*, vol. 6, no. 1, pp. 207–214, 2017.

[23] N. S. Girão, M. Muller, and L. V. R. De Arruda, "A New Biometric Identification System Based on Plantar Pressure," *IEEE Sensors Journal*, vol. 23, no. 15, pp. 16900–16906, 2023. [Online]. Available: https://ieeexplore.ieee.org/document/10155638/

[24] A. G. Leal-Junior, A. Frizera, L. M. Avellar, C. Marques, and M. J. Pontes, "Polymer Optical Fiber for In-Shoe Monitoring of Ground Reaction Forces During the Gait," *IEEE Sensors Journal*, vol. 18, no. 6, pp. 2362–2368, 2018. [Online]. Available: http://ieeexplore.ieee.org/document/8268077/

[25] M. A. Kamizi, L. H. Negri, J. L. Fabris, and M. Muller, "A Smartphone Based Fiber Sensor for Recognizing Walking Patterns," *IEEE Sensors Journal*, vol. 19, no. 21, pp. 9782–9789, 2019. [Online]. Available: https://ieeexplore.ieee.org/document/8756298/

[26] K. Alemdar, S. Likoglu, K. Fidanboylu, and O. Toker, "A novel periodic macrobending hetero-core fiber optic sensor embedded in textiles," in *2013 8th International Conference on Electrical and Electronics Engineering (ELECO)*, pp. 467–471, 2013. [Online]. Available: http://ieeexplore.ieee.org/document/6713886/

[27] A. Moraleda, C. García, J. Zaballa, and J. Arrue, "A Temperature Sensor Based on a Polymer Optical Fiber Macro-Bend," *Sensors*, vol. 13, no. 10, pp. 13076–13089, 2013. [Online]. Available: http://www.mdpi.com/1424-8220/13/10/13076

[28] K. V. Madhav, Y. Semenova, and G. Farrell, "Macro-bend optical fiber linear displacement sensor," in *Optical Sensing and Detection*, vol. 7726, p. 772608, 2010. [Online]. Available: https://doi.org/10.1117/12.854631

[29] P. Wang, Y. Semenova, Q. Wu, and G. Farrell, "A fiber-optic voltage sensor based on macrobending structure," *Optics & Laser Technology*, vol. 43, no. 5, pp. 922–925, 2011.

[30] C.-C. Chiang and J.-C. Chao, "Whispering gallery mode based optical fiber sensor for measuring concentration of salt solution," *Journal of Nanomaterials*, vol. 2013, 2013. [Online]. Available: https://doi.org/10.1155/2013/372625

[31] P. Wang, Y. Semenova, Q. Wu, G. Farrell, Y. Ti, and J. Zheng, "Macrobending single-mode fiber-based refractometer," *Applied Optics*, vol. 48, no. 31, pp. 6044–6049, 2009.

[32] W. Chen, Y. Zhang, W. Zhang, Q. Chen, Y. Zhang, M. Li, W. Zhao, Y. Zhang, and T. Yan, "High-sensitive tilt sensor based on macro-bending loss of single mode fiber," *Optical Fiber Technology*, vol. 50, pp. 1–7, 2019.

[33] M. A. Kamizi, D. Lugarini, R. Fuser, L. H. Negri, J. L. Fabris, and M. Muller, "Multiplexing Optical Fiber Macro-Bend Load Sensors," *Journal of Lightwave Technology*, vol. 37, no. 18, pp. 4858–4863, 2019. [Online]. Available: https://ieeexplore.ieee.org/document/8742655/

[34] V. de Carvalho, A. E. Lazzaretti, J. L. Fabris, and M. Muller, "Pressure-sensitive platform based on multiplexed in-series macro-bend optical fiber sensors," *Applied Optics*, vol. 62, no. 8, pp. C1–C7, 2023. [Online]. Available: https://opg.optica.org/ao/abstract.cfm?URI=ao-62-8-C1

[35] R. O. Duda, P. E. Hart, and D. G. Stork, *Pattern Classification*, 2nd ed. New York: Wiley, 2001.

[36] I. T. Jolliffe and J. Cadima, "Principal component analysis: a review and recent developments," *Philosophical Transactions of the Royal Society A: Mathematical, Physical and Engineering Sciences*, vol. 374, no. 2065, p. 20150202, 2016. [Online]. Available: https://royalsocietypublishing.org/DOI/10.1098/rsta.2015.0202

[37] L. Sunitha and M. B. Raju, "Multi-class classification for large datasets with optimized SVM by non-linear kernel function," *Journal of Physics: Conference Series*, vol. 2089, no. 1, p. 012015, 2021. [Online]. Available: https://iopscience.iop.org/article/10.1088/1742-6596/2089/1/012015

[38] S. Buttcher, C. L. A. Clarke, and G. V. Cormack, *Information retrieval: implementing and evaluating search engines*. Cambridge, Mass: MIT Press, 2010.